Dynamic analysis of a pile-supported wharf utilizing a three-dimensional numerical method

Nghiem Xuan Tran, Sung-Ryul Kim
Dept. of Civil Engineering – Dong-A University, Busan, South Korea
Jin-Sun Lee
Dept. of Civil and Environmental Engineering – WonKwang University, Iksan, Jeonbuk, South Korea

ABSTRACT
Aseismic designs of pile-supported wharves are commonly performed utilizing simplified or simplified dynamic analyses, such as multi-mode spectral or push-over analyses, respectively. Simplified analyses can be useful for evaluating the limit state of structures. However, several pile-supported wharves that were damaged during past earthquakes have shown that soil deformation and soil–pile dynamic interaction significantly affect the entire behavior of structures. Such behavior can be captured by performing dynamic analyses, which can properly consider the dynamic interactions among the soil–pile–structure. The present study attempts to investigate the earthquake performance of a pile-supported wharf utilizing a three-dimensional numerical method. The damaged pile-supported wharf at the Kobe Port during the Hyogo-ken Nambu earthquake (1995) is selected to understand the seismic behavior of the wharf and the importance of soil–structure dynamic interactions. Analysis results show a suitable agreement with the observations on the damaged wharf, and the significant effect of pile–soil dynamic interaction on the seismic performance of the wharf.

1. Introduction

A pile-supported wharf among in-front water structures can be an effective structure for transmitting a large load to a strong bearing stratum. A wharf comprises a deck and its supporting piles that are constructed on a dike (Iai, 1998). The pile-supported wharf generally exhibits three failure causes during an earthquake: the inertia force from the deck weight, large movement from a retaining wall and lateral displacement of the supporting ground (Iai 1998; PIANC, 2001).

The conventional design philosophy for pile-supported wharves under dynamic conditions shows that the seismic load is converted into an equivalent static load through a coefficient of horizontal loading related to the maximum magnitude of the shaking motion (PIANC, 2001; OCDI, 2009; ASCE, 2014). The maximum shaking magnitude of an excitation is computed based on the seismic hazard investigation, and the design is then performed to ensure that the structure is stable under the equivalent static loading condition. Thus, the force equilibrium is the main target of the conventional method. A significant drawback of these methods, which have been acquired from research on damaged structures during strong earthquakes, is the unknown behavior of the wharf when the limit load has exceeded (i.e., deformation behavior).

Seismic performance-based design (SPBD) is an emerging method that has been developed to acquire both the force and deformation behavior of structures under seismic excitation (Iai, 2001; PIANC, 2001). A few researchers have analyzed the seismic performance of pile-supported wharves by utilizing finite element or finite difference methods.

Donahue et al. (2005) performed three-dimensional (3D) modeling and investigated the soil–pile–structure interaction of a berth at Oakland during the Loma Prieta earthquake in 1989. The connection between the pile and soil was modeled as elastic–plastic non-linear link elements. The wharf damage in the past earthquake was successfully simulated by the authors. However, the model did not consider the effect of slope deformation on the piles.

McCullough (2003), and Dickenson and McCullough (2005) performed a series of two-dimensional (2D) simulations of pile-supported wharves located at several ports. Their modeling simulated pile–soil interaction by utilizing springs. The residual displacement of the deck, acceleration response of the modeling and development of excess pore water pressure (EPWP) were properly simulated, whereas the maximum moment responses in the piles were considerably overestimated. The authors stated that the prediction in the moment response could be improved by considering the dissipation of EPWP properly, and modeling the near-pile soil behavior and an alternative constitutive law.

Na et al. (2009) established fragility curves for a pile-supported wharf at a port by performing 2D numerical analysis and considering the uncertainty of input parameters. Their results show that evaluating the residual displacement of a pile–deck system in a specific condition of ground motion and ground properties was possible.

Lu (2006) and Lu et al. (2011) developed a new parallel nonlinear finite element formulation to deal with a large-scale modeling of geotechnical issues under earthquake scenarios. Their model has been still calibrated for various conditions. A simulation of an idealized model of a pile-supported wharf was conducted. The results show that wharf displacement was significantly affected by slope characteristics and the properties of the bearing stratum. However, the absence of a gap between the pile and the ground that occurred under large deformation was identified as a direction for further studies.

As previously mentioned, most studies on pile-supported wharves have been conducted by using 2D analyses, which do not properly simulate the soil–pile–structure dynamic interaction. Moreover, the SPBD for pile-supported wharves is still a critical challenge for either

researchers or practitioners. Therefore, the present study attempts to investigate the earthquake performance of a pile-supported wharf and analyze the dynamic interactions among the soil–pile–structure by performing 3D finite difference analyses. The damaged pile-supported wharf at Kobe Port during the Hyogo-ken Nambu earthquake (1995) is selected to understand the seismic behavior of the wharf.

2. Case history: Takahama (Kobe) wharf

The well-documented damaged Takahama Wharf was selected for the analyses in this study. Figure 1 shows the location of the wharf at Kobe Port. After the Hyogo-ken Nambu earthquake (Great Hanshin earthquake) of 1995 in Japan, the deck was displaced in the seaward direction at approximately 1.3–1.7 m, as shown in Fig. 2. The pile buckling occurred at the pile head and at the points where the pile thickness changed.

Figure 2 shows that a concrete deck slab was supported by beams and piles with an outer diameter of 700 mm. The pile toe penetrated into the gravel and stiff clay stratum. The retaining wall made of concrete cellular blocks was laid on loose sand with an SPT N-value of approximately 15. A liquefiable sandy fill with an SPT N-value of approximately 10 was reclaimed behind the wall. A rubble mound was constructed at the front and back of the retaining wall for support during earthquakes. Several studies, which are summarized in the following sections, have been conducted to simulate the behavior of the Takahama Wharf.

Iai (1998) applied the effective stress analysis approach to examine the behavior of the Takahama Wharf under the Hyogo-Ken Nambu earthquake of 1995. The seismic performance of the wharf was investigated through 2D modeling. The interaction between the pile and ground was modeled as a linear spring. The author showed that the development of EPWP in the backfill soil had an important role in the large deformation of the wharf.

Ishida et al. (2002) adopted the 2D finite element method and reported that the horizontal bearing capacity of a wharf under static conditions decreased with the increase in earth pressures on piles. Minami et al. (2002) investigated the damage behavior of a wharf through push-over and dynamic nonlinear analyses. The authors also confirmed that the main causes of the wharf damage were the development of inertia force and large seaward movement of the retaining wall.

Takahashi (2002, 2003), and Takahashi and Takemura (2005) conducted a series of centrifuge model tests and 2D–3D combined simulation to acquire a comprehensive understanding of the seismic behavior of the Takahama Wharf. The researchers determined that the EPWP in the loose sand layers was the main cause of the large movement of the retaining wall and rubble mound. The movement of the retaining wall then accelerated the horizontal seaward displacement of the deck, and the movement of the rubble mound induced a large bending moment on the piles.

Although many studies have been performed to analyze the damage on the Takahama Wharf, a full 3D numerical simulation of the case has not been conducted. Therefore, 3D numerical analyses were performed in the present study to thoroughly investigate the seismic behavior of the Takahama Wharf during the Hyogo-ken Nambu earthquake of 1995.

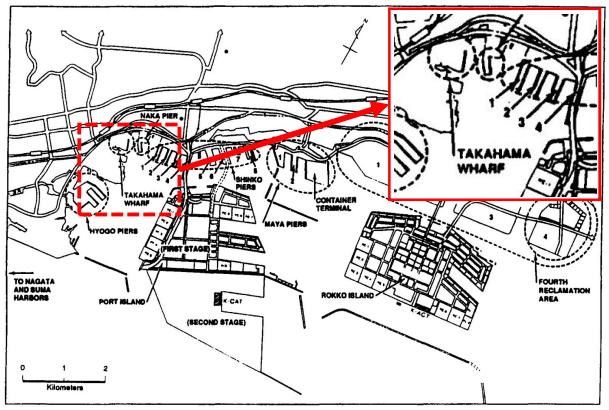

Fig. 1. Location of Takahama wharf at Kobe port (extracted from Werner et al. (1997))

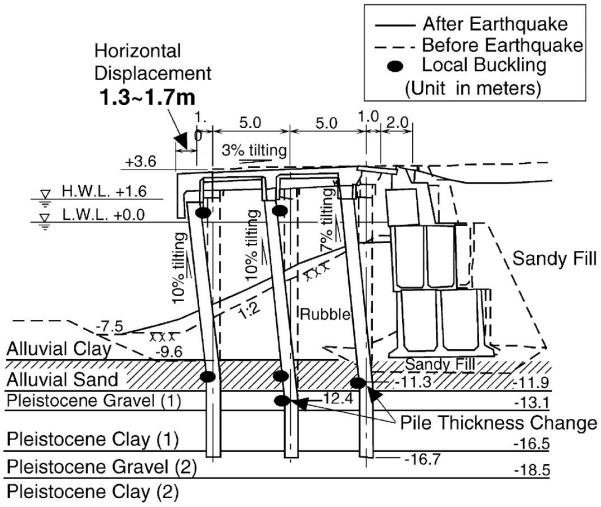

Fig. 2. Damage observation of Takahama wharf (extracted from PIANC (2001))

3. Numerical modeling

A segment of the Takahama Wharf was modeled utilizing the FLAC3D software, as shown in Fig. 3. A deck was supported by 15 piles distributed in 3 rows and 5 columns. The deck was also reinforced by three longitudinal and five normal beams. The bottom boundary of the model was determined at a depth of 28.4 m, at which the ground motion was recorded at a nearby site. The base was assumed to be a rigid layer given the large stiffness of the bearing stratum in this study. Horizontal boundaries were extended 100 m away from the slope toe and retaining wall.

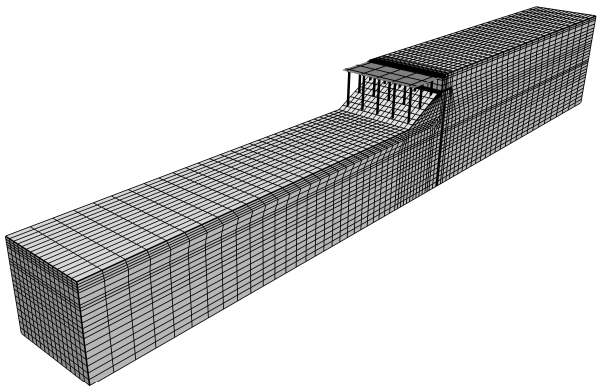

Fig. 3. Finite zones of Takahama wharf

The maximum zone size of approximately 1.5 m in the vertical direction was applied to ensure the proper transmission of the shear wave following the relation in Eq. 1 (Itasca, 2012). The C_s value was approximately 220 m/s in the equation, as determined by the average shear velocity of the ground. The zone size was gradually increased from the wharf to the boundaries in the horizontal direction for computational efficiency. The length of the pile elements was set at 0.8 m to guarantee the appropriate interaction between each pile and the corresponding soil elements.

$$f_{max} = \frac{C_s}{10\Delta z} \quad [1]$$

where C_s is average shear velocity, f_{max} is the maximum frequency of ground motion after filtering, and Δz is the maximum size of the modeling in the vertical direction.

The wharf deck was modeled in this study as a shell element with a density of 2 t/m^3, thickness of 0.3 m, and Young's modulus of 50 GPa. The piles and beams were modeled by the pile and beam elements, respectively. The pile had an outer diameter of 0.7 m and a length of 20 m. The pile thicknesses were 10 mm (seaside row), 12 mm (center row), and 14 mm (landside row). The center thickness and landside piles were decreased to 9 mm at a depth of 12.4 m and 11.3 m, respectively. The yield stress of piles (SKK400) was about 235 MPa. Piles would show the yielding behavior in accordance with their reference values during simulation. The dimensions of the normal and longitudinal beams were 70 cm × 90 cm and 135 cm × 90 cm, respectively. The connection at the deck, including the pile and beam, was assumed to be rigid.

An elastic–perfectly plastic Mohr–Coulomb model was adopted to simulate the soil behavior. Table 1 lists the soil properties obtained based on the research of Iai (1998). A Finn/Byrne model of Eq. 2 was applied to the sandy fill and alluvial sand to simulate the development of EPWP. Thus,

$$\frac{\Delta\epsilon_{vd}}{\gamma} = C_1 \exp\left(-C_2 \frac{\Delta\epsilon_{vd}}{\gamma}\right) \quad [2]$$

where $\Delta\epsilon_{vd}$ is the change in volume strain, γ is the unit weight (tf/m^3), and C_1 and C_2 are the constants, which can be determined based on the relative density D_r or the corrected SPT $(N_1)_{60}$ value in the Eqs. 3 and 4 (Byrne 1991).

$$C_1 = 7600(D_r)^{-2.5} = 8.7[(N_1)_{60}]^{-1.25} \quad [3]$$

$$C_2 = \frac{0.4}{C_1} \quad [4]$$

The interaction between the pile and soil was simulated by shear and normal coupling springs. Each spring was specified by four parameters: spring stiffness, cohesive strength, friction angle, and exposed perimeter. The effective confining stress plays an important role in the strength behavior of the spring. The development of a gap at the soil–pile interface can be properly simulated.

The friction angle of the interface was considered as two-thirds of the friction angle of the corresponding soil layer. The cohesive strength of the interface was set as the cohesion of adjacent soils. Equations 5 and 6 show the determination of the normal and shear stiffness of the interface spring, respectively (Itasca, 2012).

$$k_n = \frac{2\pi K}{10\times\ln\left(1+\frac{2t}{D}\right)} \quad [5]$$

$$k_s = \frac{2\pi G}{10\times\ln\left(1+\frac{2t}{D}\right)} \quad [6]$$

where k_s is shear spring stiffness, k_n is normal spring stiffness, t is pile thickness, and D is pile diameter.

Table 1. Soil properties of the modeling

Soil layers	Density ρ, t/m^3	Bulk modulus K, MPa	Shear modulus G, MPa	Friction angle ϕ, deg	Cohesion c, MPa
Sandy fill	1.80	108.0	40.5	37	--
Alluvial sand	1.85	192.0	72.0	38	--
Alluvial clay	1.60	25.6	9.6	25	--
Pleistocene sand (1), (2)	1.85	456.0	171.0	40	--
Pleistocene clay (1), (2)	1.65	408.0	153.0	--	0.2
Rubble-mound	2.00	456.0	171.0	40	--
Retaining wall	2.10	1.14 x 10^4	1.05 x 10^4	--	--

The effects of the retaining wall on the deformation behavior of the wharf were represented by an approach bridge. The connection between the approach bridge and structures was established to transmit only the compressive axial force from the retaining wall to the deck. The characteristics of the Coulomb-type interface, which allows separation and slippage, were applied to the retaining wall.

The interface characteristics were composed of the shear and normal components. Each component was modeled by the strength and stiffness. The stiffness was determined based on the stiffness of the adjacent soil and the smallest width of an interface zone in the normal direction, as shown in Eq. 7 (Itasca, 2012). The interface friction angle was 30° at the interface of each wall block. The interface angle between the wall and adjacent soils at the bottom and side were set at 30° and 15°, respectively, following the suggestions of Alyami et al. (2007), and Dakoulas and Gazetas (2008).

$$k_{si} = k_{ni} = 10 \times \left\{ \max \left[\frac{\left(K + \frac{4}{3}G\right)}{\Delta z_{min}} \right] \right\} \quad [7]$$

where k_{si} is the shear stiffness of the interface, k_{ni} is the normal stiffness of the interface, and Δz_{min} is the smallest width of an interface zone in the normal direction.

The input ground motions at a depth of 28.4 m were obtained from the research of Iwasaki and Tai (1996). The recorded earthquake motions in the east–west and north–south directions were modified considering the face angle of the Takahama Wharf, which was inclined by approximately 20° from the north direction. The acceleration time history was processed by applying a low-pass filtering of the 10 Hz frequency regarding the major energy concentration and baseline correction. Figure 4 shows the input base motions of the normal and longitudinal directions from the wharf face.

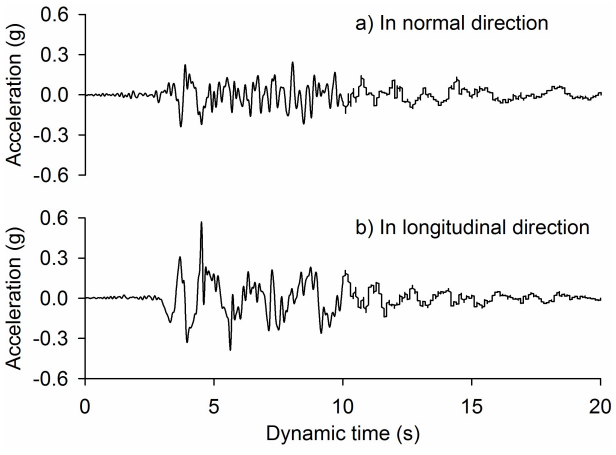

Fig. 4. Input earthquake motions at depth of 28.4 m

Hysteretic damping was applied to the model aside from the energy dissipation from the plastic deformation. A series of sigmoidal formulations with four parameters were computed to fit the stiffness degradation curves reported by Fujikawa and Fukutake (2001). A Rayleigh damping ratio of 2% was employed to remove the high-frequency noise.

A coupled mechanical–fluid simulation of the seismic behavior of the Takahama Wharf was performed in three steps. First, the wharf system was brought to the equilibrium of force to replicate the in-situ stress condition. Second, the construction stage was processed by inserting structure elements. Finally, the input earthquake motion was applied to the model base. The free field condition, which allows lateral ground motion at the boundaries, was also applied in this step.

The total element number was approximately 46,000, excluding the number of the structural elements. The analysis was completed within approximately 33 hours utilizing a total of 12 processors in a Core i7 computer.

4. Seismic behavior of Takahama wharf

Figure 5 shows the accelerations at the ground surface obtained from the numerical simulation. A peak ground acceleration of approximately 0.70 g was slightly higher than the recorded value of 0.53 g. The center frequency was obtained in this analysis by examining the undamped analysis and calculating the natural period of the entire system. However, the input properties of Rayleigh damping were not sufficiently reasonable to remove the high-frequency noise, as shown in Fig. 5.

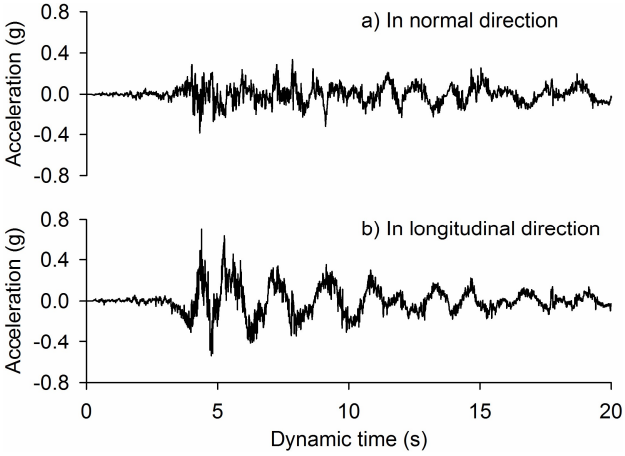

Fig. 5. Surface acceleration response

Figure 6 presents the residual seaward displacement of the wharf at the end of the shaking. The top of the retaining wall, the approach bridge, and the deck moved together at a distance of approximately 1.56–1.63 m in the seaward direction. The ground surface was heaved up in front of the slope and settled down at the back of the wall, as shown in Fig. 6. The clay layer moved up by approximately 0.48 m at the area near the slope toe. Conversely, the settlement

of the sandy fill behind the retaining wall was approximately 1.15 m and decreased gradually to 0.1 m at the boundary, as shown in Fig. 7.

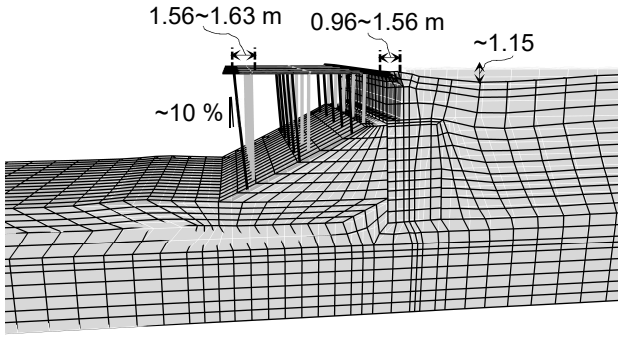

Fig. 6. Deformed shape of Takahama wharf after the end of earthquake (magnified by a factor of two)

Figure 7 shows the lateral movements of the slope and wall, as well as the settlement of the backfill soil. The peak displacement of the wall ranged from 0.99–1.60 m, and the wall tilting was approximately 4.6%. The peak movement of the slope was approximately 1.16–1.50 m, which increased gradually from the top to the toe. The tilting of the retaining wall may have caused the smaller seaward movement of the rubble layer as against the deck. The residual movement of the slope toe was almost similar to that of the wall and alluvial sand. This scenario implies that the piles did not prevent the seaward movement of the slope from the strong shaking.

The buckling phenomenon likely occurred on all piles at depths of 12.3–12.9 m, which were immediately below the alluvial sand, as shown in Fig. 8. The bending moment may have been induced by the inertia force of the deck and the kinematic deformation of the retaining wall. This observation agrees with the measured buckling points of the center piles. However, the buckling for the seaside and landside piles was located approximately 1.0 m deeper than the recorded value at approximately the middle of the alluvial sand layer (11.3 m). All piles were tilted by approximately 10%, which were almost the same as the observed data.

The numerical simulation successfully captured quantitatively and qualitatively the overall behavior of the Takahama Wharf during Hyogo-ken Nambu earthquake of 1995. The major concerns in the current subject, which are the effects of the development of EPWP and approach bridge, are discussed below.

The soil softening caused by the development of EPWP during shaking was considered as the main reason for the large deformation of the structures under the strong motion. The behavior of the effective stress and the development of EPWP were monitored during the shaking in this study.

The EPWP ratio r_u, which is defined as the ratio of the EPWP to the initial effective vertical stress, increased rapidly after approximately 5 s, as shown in Fig. 9. Consequently, the wharf moved together with the ground until approximately 5 s at the early stage. The seaward movement of the wharf increased considerably with the rapid development of EPWP, as shown in Fig. 7. Although complete liquefaction was not observed, the peak value of the r_u was approximately 0.85, and the development of the excess pore pressure induced the rapid increase in earth pressure on the wall. Similar results were observed from previous numerical studies and experimental tests. Although several parts near the surface were liquefied, complete liquefaction did not occur at the alluvial sand layer and slope, as reported by Minami et al. (2002), and Takahashi and Takemura (2005).

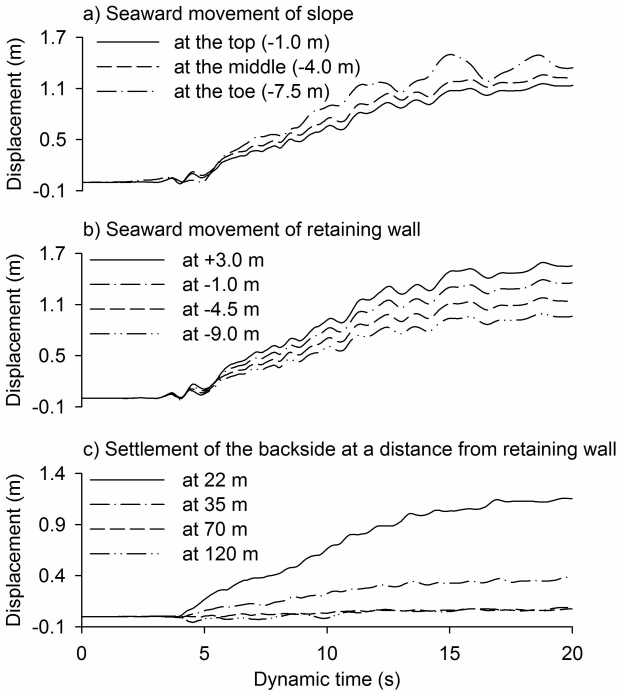

Fig. 7. Time histories of residual displacement of individuals of wharf model

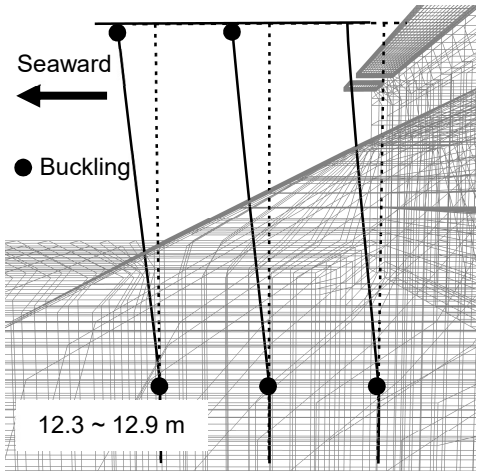

Fig. 8. Residual bending curvature of center pile column

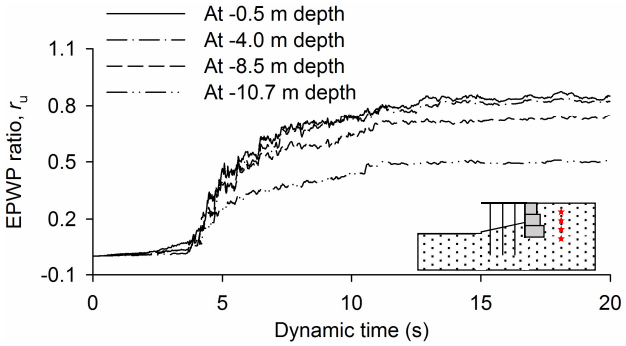

Fig. 9. Development of EPWP at several depths

The analysis of the seismic behavior of the wharf without considering the development of EPWP was conducted by applying only the Mohr–Coulomb model to the liquefiable soil layers. The results showed that the wharf moved by approximately 0.52 m toward the sea, which was significantly smaller than the observed deformation. All structures remained in their elastic condition. The rapid development of EPWP was again the major cause for the large seaward movement of the wharf.

Moreover, the effect of the approach bridge, which connects the deck and the wall, was numerically analyzed. The retaining wall showed a higher seaward displacement of 0.04 m in the absence of the approach bridge, whereas the deck moved laterally at 0.38 m, which was significantly smaller than the observation. The pile material remained in the elastic condition for this analysis. Therefore, the approach bridge had a governing effect on the seaward movement of the deck system. The wharf pushed back with a force to restrain the displacement of the retaining wall through the bridge.

5. Summary and conclusion

This study attempted to understand the seismic behavior of a wharf at Kobe Port during a past earthquake. Several significant aspects were determined by utilizing the 3D finite difference analysis.

The seaward displacement of the Takahama Wharf can be successfully simulated by numerical analysis. The prediction of the displacement, tilting, and pile buckling of the entire modeling conformed with the measured data.

By applying bidirectional ground motions in the 3D modelling, it is possible to simulate the behavior of EPWP development during strong earthquake. Although liquefaction did not occur, the rapid development of EPWP in the two liquefiable soil layers was the main cause for the large deformation observed. The kinematic energy of the retaining wall movement resulted in the corresponding seaward movement of the deck through an approach bridge. Thus, the approach bridge had a significant effect on the seismic behavior of the wharf system.

The crack on the approach bridge was ignored in this study. The connection between the deck and piles was also not treated carefully such as in actual conditions. These uncovered aspects can be addressed in future studies.

Acknowledgment

This research was supported by the project entitled "*Development of performance-based seismic design technologies for advancement in design codes for port structures,*" funded by the Ministry of Oceans and Fisheries of Korea and Basic Science Research Program funded by the Ministry of Education (NRF-2016R1A6A1A03012812).

Reference

Alyami, M., Wilkinson, S.M., Rouainia, M. and Cai, F. 2007, June. Simulation of Seismic Behavior of Gravity Quay Wall using a Generalized Plasticity Model, 4th International Conference on Earthquake Geotechnical Engineering, Thessaloniki, Greece, No. 1734.

ASCE 2014. *Seismic Design of Piers and Wharves (61-14)*, American Society of Civil Engineers.

Byrne, P. 1991. A Cyclic Shear-Volume Coupling and Pore-Pressure Model for Sand, *2nd International Conference on Recent Advances in Geotechnical Earthquake Engineering and Soil Dynamics*, The University of Missouri-Rolla, USA, No. 1.24: 47–55.

Dakoulas, P. and Gazetas, G. 2008. Insight into Seismic Earth and Water Pressures against Caisson Quay Walls, *Geotechnique*, 58(2): 95–111.

Dickenson, S.E. and McCullough, N.J. 2005. Modeling the Seismic Performance of Pile Foundations for Port and Coastal Infrastructure, *Workshop on Seismic Performance and Simulation of Pile Foundations in Liquefied and Laterally Spreading Ground,* ASCE, University of California, Davis, California, United States, 173–191.

Donahue, M. J., Dickenson, E. S., Miller, T. H., and Yim, S. C. 2005. Implications of the Observed Seismic Performance of a Pile-Supported Wharf for Numerical Modeling, *Earthquake Spectra*, 21, 617–634.

Fujikawa S and Fukutake, K. 2001. Simulation of the Vertical Seismic Array Records at the Kobe Port Island Considering the Effect of the Improved Ground Adjacent to the Array Site, *Journal of JSCE,* Japan Society of Civil Engineers, 687(III-56): 169–80.

Iai, S. 1998. Seismic Analysis and Performance of Retaining Structures, *Geotechnical Earthquake Engineering and Soil Dynamics III*, ASCE, Seattle, Washington, USA, 1020–1044.

Iai, S. 2001. Seismic performance-based design of port structures and simulation techniques, *International Workshop on Earthquake Simulation in Geotechnical Engineering*, Case Western Reserve University Cleveland, Ohio, USA, 1–12.

Iai, S. *Personal Communication*, 2016.11.26–2016.11.28.

Ishida, M., Ueda, S., Ikeuchi, T., and Suzuki, T. 2002. Assessment of Pier Pile Failure Resulting from 1995 Kobe Earthquake, *12th International Offshore and Polar Engineering Conference*, The International Society of Offshore and Polar Engineers, Kitakyushu, Japan, 552–559.

Itasca 2012. FLAC3D Version 5.00 Fast Lagrangian Analysis of Continua in 3 Dimensions, *User's Manual*, Itasca Consulting Group, Inc., Minneapolis, Minnesota, USA.

Iwasaki, Y. and Tai, M. 1996. Strong Motion Records at Kobe Port Island. *Special Issue of Soils and Foundations*, Japanese Geotechnical Society, 29–40.

Lu, J. 2006. *Parallel Finite Element Modeling of Earthquake Site Response and Liquefaction*, Ph.D. Dissertation, University of California, San Diego, USA.

Lu, J., Elgamal, A., Yan, L., Law, K.H. and Conte, J.P. 2011. Large-Scale Numerical Modeling in Geotechnical Earthquake Engineering, *International Journal of Geomechanics*, ASCE, 11(6): 490-503.

McCullough, N. J. 2003. *The Seismic Geotechnical Modeling, Performance, and Analysis of Pile-Supported Wharves*, Ph. D. Dissertation, Oregon State University, Corvallis.

Minami, K., Yokota, H., Sugano, T., and Kawabata, N. 2002. Damage Investigation and Structural Analysis of Piled Berthing Structures during 1995 Hyogoken-Nambu Earthquake, *12th International Offshore and Polar Engineering Conference*, The International Society of Offshore and Polar Engineers, Kitakyushu, Japan, 507–513.

Na, U. J., Chaudhuri, S. R., Shinozuka, M. 2009. Performance Evaluation of Pile-Supported Wharf under Seismic Loading, *TCLEE 2009*, Lifeline Earthquake Engineering in a Multihazard Environment, Oakland, 1032–1041.

OCDI 2009. *Technical Standards and Commentaries for Port and Harbor Facilities in Japan,* The Overseas Coastal Area Development Institute of Japan.

PIANC 2001. *Seismic Design Guidelines for Port Structures,* Permanent International Navigation Association, A.A. Balkema Publishers, Rotterdam, Netherlands.

Takahashi, A. 2002. *Soil–Pile Interaction in Liquefaction-Induced Lateral Spreading of Soils,* DEng Thesis, Tokyo Institute of Technology, Japan.

Takahashi, A. 2003. Seismic Performance Evaluation of Pile-Supported Wharf by 3D Finite Element Analysis, *12th Asian Regional Conference on Soil Mechanics and Geotechnical Engineering*, Meritus Mandarin, Singapore, 1: 245–8.

Takahashi, A. and Takemura, J. 2005. Liquefaction-induced Large Displacement of Pile-Supported Wharf, *Soil Dynamics and Earthquake Engineering*, 25(11): 811–825.

Werner, S.D., Dickenson, S.E. and Taylor, C.E. 1997. Seismic Risk Reduction at Ports: Case Studies and Acceptable Risk Evaluation, *Journal of Waterway, Port, Coastal, and Ocean Engineering*, 123(6): 337–346.